

Validation of three-dimensional total knee replacement kinematics measurement using single-plane fluoroscopy

R. Daems¹, J. Victor², P. De Baets³, S. Van Onsem² and M.A. Verstraete²

¹Ghent University, Belgium

²Ghent University, Department of Physical Medicine and Orthopaedic Surgery, Belgium

³Ghent University, Laboratory Soete, Belgium

Abstract: Instability of the knee after total knee arthroplasty (TKA) is today the number one reason for aseptic revision surgery. In vivo evaluation of knee kinematics using single-plane fluoroscopy has become an important method to investigate knee stability and compare different implant designs. A validation experiment was performed to assess the accuracy of this method. A total knee implant was installed on sawbones and a flexion extension movement was performed with the sagittal plane parallel to the detector panel of the fluoroscope. Simultaneously, the sawbones were tracked using a conventional motion tracking system and rigidly attached markers. That measurement can be seen as a golden standard and is therefore believed to represent the real positions.

The results indicate that knee rotations can be measured with an accuracy of approximately 0.6° and sagittal plane translations can be measured with an accuracy of approximately 0.4 mm. These results prove that the method is sufficiently accurate for clinical use.

Keywords: single-plane X-ray fluoroscopy, 2-D to 3-D registration, total knee arthroplasty, kinematics

1 Introduction

Total knee arthroplasty (TKA) involves a replacement of the knee joint with artificial implants. The implants typically consist of two metallic components installed on the tibia and femur, with a high molecular weight polyethylene insert in between.

The number of TKA's performed each year in the United States is projected to grow rapidly, from 600,000 in 2005 to 3.5 million by 2030 [1]. Knee instability has nowadays become the number one

reason for aseptic TKA revisions [2].

These two factors indicate the importance of accurate methods to evaluate in vivo knee kinematics. Through these measurements, insight is provided in the implant characteristics that can ultimately help designing future implants. To that extent, a large number of patients with different knee implants needs to be analyzed, linking the kinematic data to the patient satisfaction levels.

Single-plane fluoroscopy is a non-invasive in vivo method that is widely used for this purpose [3–6]. High accuracies have been reported in literature, up to one degree in rotations and 0.5 mm for translations in the sagittal plane [7, 8]. However, such validation remains highly dependent on the personal skill, installed devices and used software packages. Therefore, a validation procedure is advisable for each lab performing such measurements. This paper evaluates the accuracy of the procedure at Ghent University. If the results of the validation experiment are satisfying, more detailed analyses can be performed (e.g. observing condylar contact loss [9]).

2 Methods

2.1 Validation experiment

The implant used for the validation experiment is the Journey II BCS [10] with a femoral and tibial size 5, and a poly-ethylene insert with a thickness of 10 mm. The implant is installed on medium sized, left side sawbones [11]. Sawbones are artificial bones made of a rigid foam shell with inner cancellous material. This makes them ideal for drilling and cutting, thus for installing the implants. A motion tracking system with infrared cameras is used (NaturalPoint Inc., Corvallis, OR, USA) as a golden standard for the positions of the implants. Three motion tracking spheres are rigidly attached to each bone (*figure 1*). The reader is referred to *section 2.4* for a more detailed explanation.

A flexion extension movement (-8° to 98° flexion) is performed with the sagittal plane parallel to the detection panel of the fluoroscope. The fluoroscopy images are processed by three different observers. The positions are recorded by the motion tracking system, and after post-processing compared to the single-plane fluoroscopy data. *Figure 2* shows the work-flow of the post-processing. The subsequent paragraphs explain each step in more detail.

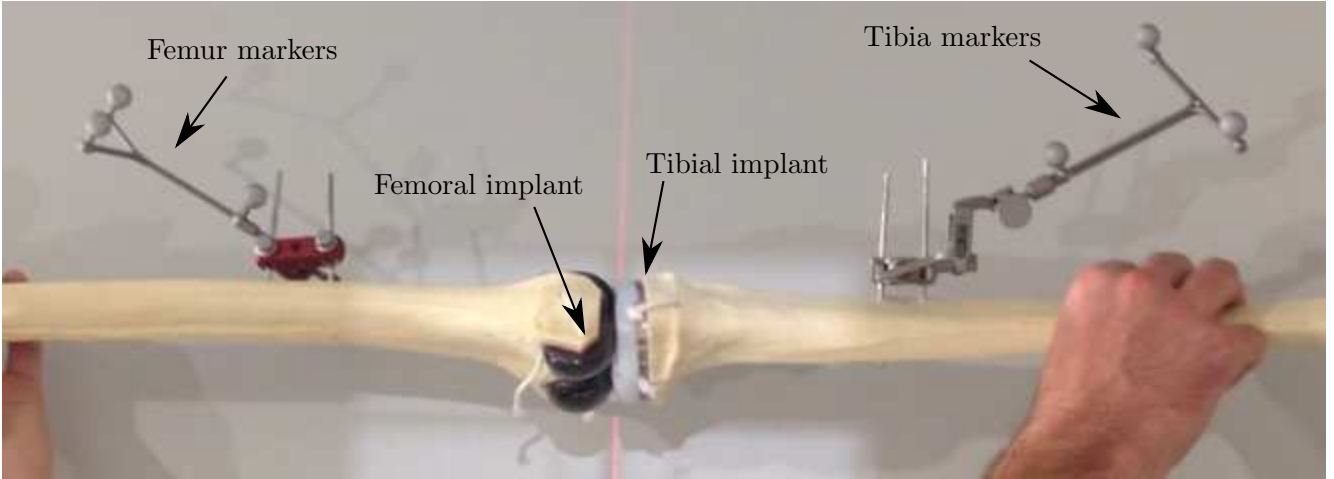


Figure 1: Sawbones with installed implants and rigidly attached motion tracking spheres.

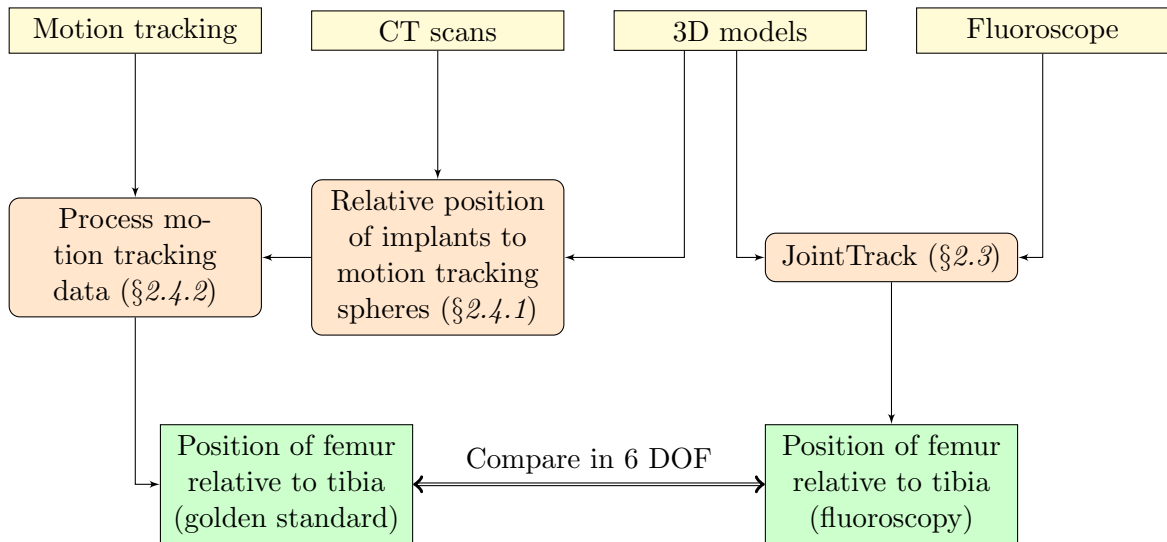


Figure 2: Flowchart of the validation experiment post-processing.

2.2 Kinematic description of knee movement

Per convention the tibia is kept in a fixed position; the femur is moving relatively to the tibia. Based on the kinematic description by Grood and Suntay [12] the six degrees of freedom of the knee joint are defined. *Figure 3* illustrates the three rotational and three translational degrees of freedom for a left knee, with the arrows pointing in the positive directions. *Table 1* lists these degrees of freedom with their clinical names, also indicating the positive and negative directions. All results presented in this paper use this definition.

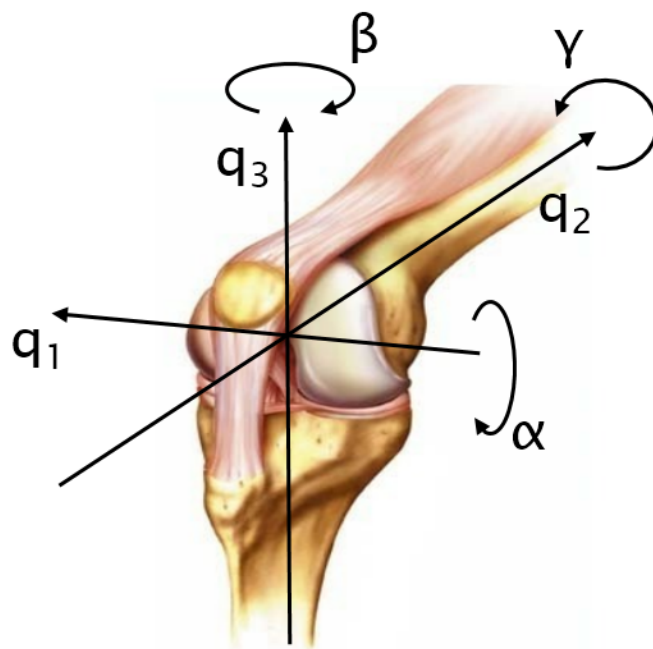


Figure 3: Degrees of freedom of the left knee.

q_1	+/-	Medial/lateral femoral displacement
q_2	+/-	Posterior/anterior femoral displacement
q_3	+/-	Joint distraction/compression
α	+/-	Flexion/extension
β	+/-	Valgus/varus
γ	+/-	Internal/external rotation

Table 1: Degrees of freedom.

2.3 Single-plane fluoroscopy

A fluoroscope registers X-ray frames at high speed. This enables visualizing real-time motion. Frames are recorded with a low shutter time, to minimize motion blurring. The fluoroscope used for the validation experiment is a Siemens Axiom Luminos dRF (Siemens Healthcare GmbH, Munich, Germany) with a frame rate of eight hertz. In *figure 4(a)* an example fluoroscopic image is shown. The metal implants are clearly visible because they are opaque to the radiation beams. Using a Canny Edge Detection algorithm [13] the contours of the implants are detected (*figure 4(b)*), subsequently the 3D models of the implants are matched on the contours (*figure 4(c)*). As a result, the 3D positions and orientations are derived from 2D images. The process of matching the 3D models on the images is performed using the open-source software package JointTrack [14].

Matching the 3D models in JointTrack is a process that involves tedious and precise manual labor. A first estimation of the positions of the 3D models has to be manually provided. Based on the estimation, an optimization algorithm will try to find an optimum by rotating and translating the 3D models in small steps. A cost function minimizes the normalized sum of the distances between the edge points of the 3D models and the edge points in the images [15].

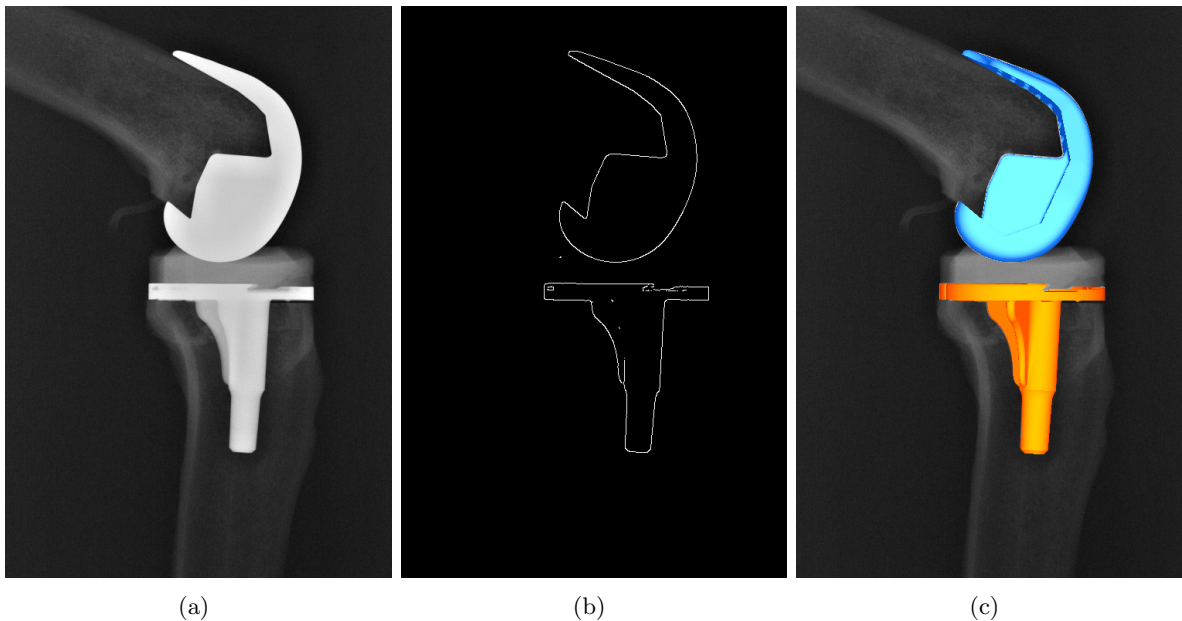


Figure 4: Fluoroscopic image (a), edge detection (b) and matching of the 3D models (c).

2.4 Golden standard: rigid body motion tracking

A motion tracking system (NaturalPoint Inc., Corvallis, OR, USA) is used as a golden standard for measuring the positions of the implants. Six infrared cameras track the positions of rigidly connected reflective spheres in space. The system measures the position of the markers 120 times per second and has an accuracy of 0.255 mm [16].

On each of the bones, a rigid structure is installed holding three reflective markers (*figure 1*). From the positions of these three markers, the position and orientation of the attached rigid structure (i.e. bone and implant) is derived.

2.4.1 Relative position of the reflective markers to the implants

However, the relative position of the bone implants to the reflective markers has to be determined. This is done using a computed tomography (CT) scan of the whole structure, for each bone. The CT scan has a voxel size of 0.6 mm. CT post-processing is done with Mimics software (Materialise NV, Leuven, Belgium).

Figure 5 depicts a slice of the CT scan, the femoral implant is clearly visible on the image. The green region is selected using thresholding, i.e. selecting regions above a certain brightness level. This way, the implant can be separated from the bone in the CT scan. Afterwards a 3D model of this part of the scan can be made (*Figure 6(a)*). The same method is applied for the three reflective markers. Subsequently on each of the reflective markers a sphere is fit, and the centers of the spheres is determined. This is done with the software 3-matic (Materialise NV, Leuven, Belgium).

Now the coordinates of the reflective markers are known relative to the 3D model of the CT scan. The next step is finding the coordinates of the reflective markers relative to the original 3D model, the same model used for the JointTrack processing. *Figure 7* shows a schematic example of that step for the femoral implant. P'_1 , P'_2 and P'_3 are the coordinates of the three reflective markers. The CT scan 3D model is now moved and rotated in space, together with P'_1 , P'_2 and P'_3 , to overlap and align with the original 3D model. This is done using a functionality in 3-matic called *Global registration*. *Figure 6* shows both 3D models after this step. Now the coordinates of the reflective markers are known relative to the original 3D model (P_1 , P_2 and P_3).

There is however a significant uncertainty in the relative positioning using this method, for the following two reasons. First, the voxel size of the CT scan is relatively large, the voxels are clearly

visible (*figure 6(a)*). Second, the metallic implant produces a large amount of glare and noise in the CT scan.

This positioning error emerges from the first results of the experiment. A significant bias was found for all degrees of freedom. *Figure 8* shows the measurement results for γ as an example. All observers estimated positions below the ones calculated using the golden standard method, through the entire range of motion. Similar phenomena are observed for the other degrees of freedom. If the relative position of the reflective markers is rotated by a correctly chosen constant, in a direction corresponding to γ to counteract this bias, the bias disappears and a more correct position is known.

To find the correctional constants for all degrees of freedom, a parametric study was performed. The position of the reflective markers is changed in steps of 0.1 mm and 0.1 degrees within a realistic range of ± 1 mm and ± 2 degrees. A cost function is calculated for all the possibilities in six degrees of freedom within these ranges. The cost function is the sum of the root mean square errors for all degrees of freedom (millimeters and degrees equally weighed). Minimizing the cost function is believed to indicate a more correct relative position of the reflective markers.

Only the relative position of the femoral reflective markers is investigated, because making a change in the relative position of the tibial reflective markers corresponds directly with a change for the femur. That is because ultimately only the relative position of the femur to the tibia is of importance. A change of position in the tibia will always correspond to an inverse change of position in the femur.

The offset derived from the parametric studie is within the proposed, realistic ranges for five out of six degrees of freedom. Only for the mediolateral translation, which corresponds mostly to the out-of-plane (z) direction, no optimum was found within the range. Therefore, no optimization in the z -direction was performed. In *Section 3.2* a bias of approximately 4 mm is introduced as possible explanation. The optimization tries to solve this bias, going further than the realistic range of ± 1 mm. No optimum within this range exists.

Table 2 shows the correctional constants for all degrees of freedom.

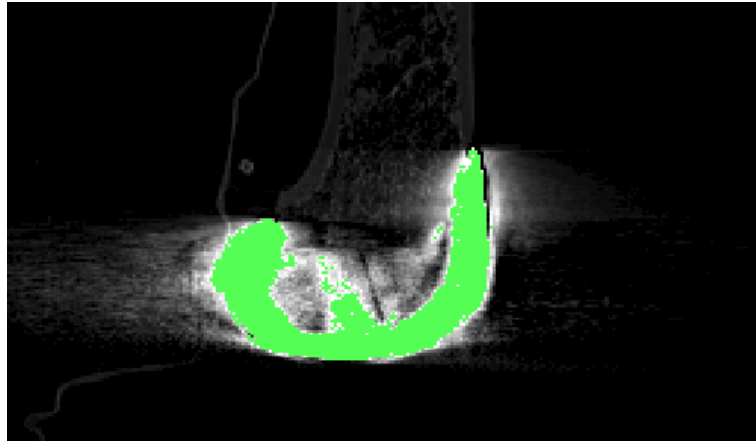


Figure 5: CT scan slice, illustrating thresholding (green) to separate metallic implant

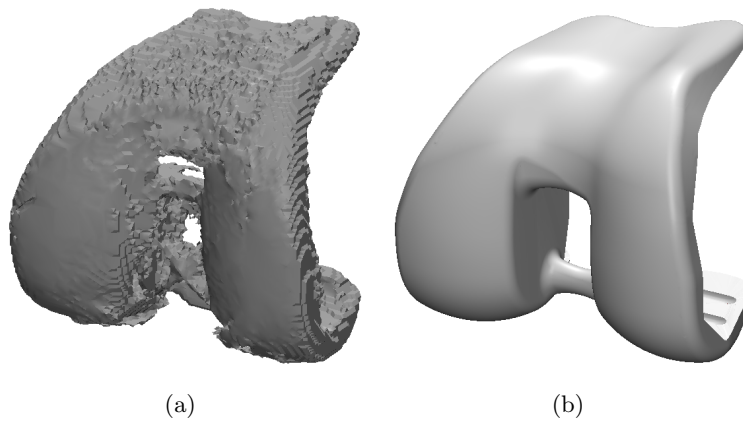


Figure 6: CT 3D model (a) and the original 3D model (b) in the same orientation

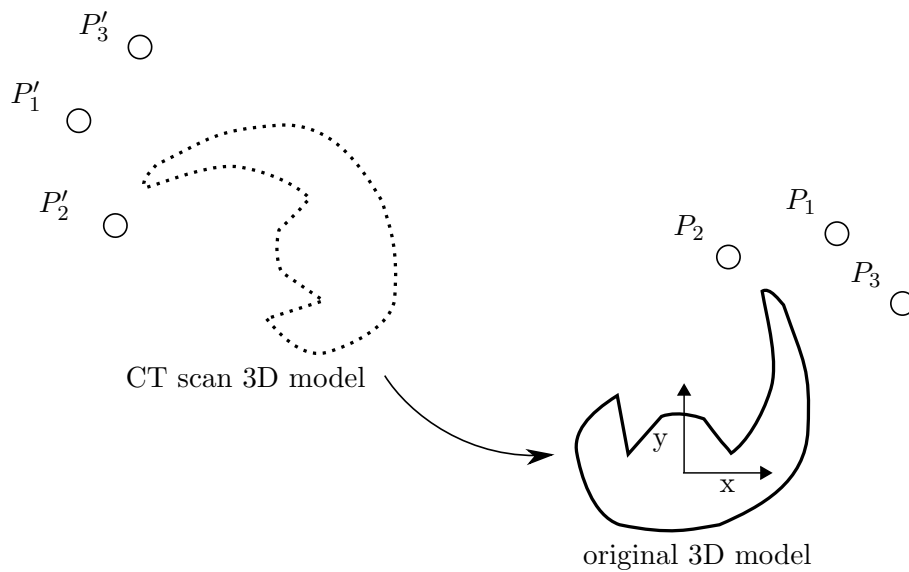


Figure 7: Using global registration, the CT scan 3D model is aligned with the original 3D model, yielding the coordinates of the reflective markers relative to the original 3D model.

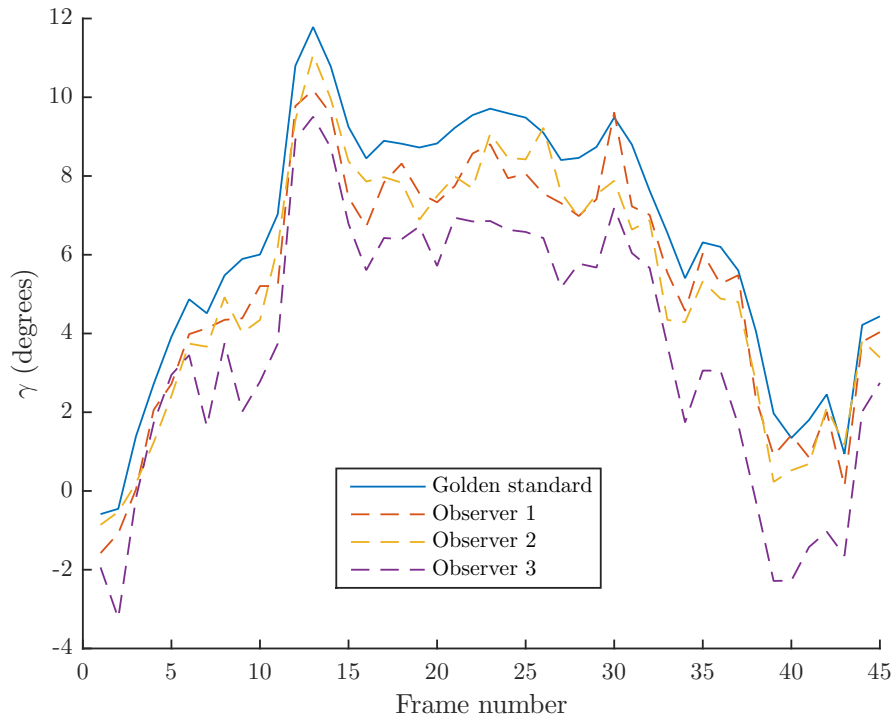


Figure 8: Results for γ illustrating the positioning error

x translation	+ 0.4 mm
y translation	- 0.2 mm
z translation	-
x rotation	- 0.7
y rotation	- 1.1 °
z rotation	- 1.3 °

Table 2: Motion tracking spheres positional correction values.

2.4.2 Deriving the relative position of the femur to the tibia

The next step is determining the relative position of the femur to the tibia for every measured moment. To that purpose a rigid transformation is estimated that puts the coordinates of the reflective markers (P_1 , P_2 and P_3) in the registered positions by the motion tracking system [17]. If that transformation is executed on the implant 3D model, it will be correctly positioned in the coordinate system of the motion tracking system. Since that is done for both the femur and tibia implant models, and only the

relative position of the femur to the tibia is important, it is not important how the motion tracking system coordinate system is orientated or where the origin is. Furthermore, if T_{femur} is the femur transformation and T_{tibia} is the tibia transformation, applying

$$T = T_{tibia}^{-1} \cdot T_{femur}$$

to the femur, will position the femur relative to the tibia, in the coordinate system of the tibia.

The kinematics can now be expressed in the six degrees of freedom defined in *section 2.2* and compared to the fluoroscopy measurements.

3 Results and discussions

3.1 Accuracy in six degrees of freedom

In *table 3* the root mean square errors are shown for all degrees of freedom. The results for the accuracy in the out-of-plane (z) direction are expected to be worst, because a movement in the z direction causes only a very small change in the contours. By moving an object along in the z direction, the object will appear somewhat smaller in the image, but this change is very small compared to movement in the in-plane direction. The z direction corresponds mostly with the q_1 degree of freedom (*section 2.2*), since a flexion extension movement in the sagittal plane is performed.

Because knee movement in the q_1 direction is minimal, it is justified to place the femoral and tibial components manually in realistic relative positions in the z direction. This is possible in JointTrack: after matching all the images a first time, settings can be adjusted so the optimization algorithm will not change the position in the z direction. If the user now moves the femoral and tibial components in realistic positions, the software can optimize again without changing the z direction. The results for this method are shown in *table 3*. q_1 is vastly improved. Note that the method has a small effect on the other degrees of freedom.

The results are excellent compared to literature [7, 8] and high enough for clinical use. A disadvantage of this experiment is that no tissue was surrounding the implants. This might have an ameliorating effect on the results, because the tissue has the potential to lower the contrast of the implants with the background in the images.

DOF	Results	manual z
q_1	4.84 mm	1.43 mm
q_2	0.37 mm	0.49 mm
q_3	0.29 mm	0.27 mm
α	0.44 °	0.34 °
β	0.57 °	0.56 °
γ	0.64 °	0.90 °

Table 3: Root mean square errors for all degrees of freedom, including manual z direction positioning.

3.2 Bias in the out-of-plane direction

A large bias was observed in the q_1 direction (+ 4 mm). This means that the JointTrack software estimates that the femur is 4 mm closer (or the tibia 4 mm further away) compared to the golden standard positions. A possible explanation is found in the different materials of the implant components. The femoral component is made of oxidized zirconium and the tibial component is made of titanium [10]. Zirconium has a higher X-ray attenuation factor than titanium [18], which means it is more opaque to X-ray beams. Furthermore, the femoral component is thicker and not contained within the bone. These factors will attribute to a higher contrast of the femoral component with the surroundings compared to the tibial component. This higher contrast creates a sharper edge in the image than the lower contrast of the tibial component. The JointTrack software uses the Canny Edge Detection algorithm [13], which will interpret this sharper edge to be somewhat bigger, i.e. the contour line is estimated to be more on the outside of the silhouette. It can be calculated that an out of plane movement of 4 mm corresponds with a decrease of 0.65 pixels of a typical cross section length of 211 pixels of the tibial component in the image. This rather small value supports the proposed explanation, although more experiments with different implants made out of different materials would be necessary to further understand this problem.

4 Conclusion

The validation experiment indicates that knee rotations can be measured with an accuracy of approximately 0.6° and sagittal plane translations can be measured with an accuracy of approximately 0.4

mm. The results are excellent compared to literature and high enough for clinical use. Manual repositioning of the implant components in the out of plane direction to a realistic relative mediolateral position proves to be an effective method to improve accuracy.

Acknowledgment

The authors would like to thank Dr. Scott Banks for the many helpful suggestions and the use of JointTrack in general.

References

- [1] S. Kurtz, K. Ong, E. Lau, F. Mowat, and M. Halpern, “Projections of primary and revision hip and knee arthroplasty in the united states from 2005 to 2030,” *J Bone Joint Surg Am*, vol. 89, no. 4, pp. 780–785, 2007.
- [2] R. S. Namba, G. Cafri, M. Khatod, M. C. Inacio, T. W. Brox, and E. W. Paxton, “Risk factors for total knee arthroplasty aseptic revision,” *The Journal of arthroplasty*, vol. 28, no. 8, pp. 122–127, 2013.
- [3] T. F. Grieco, A. Sharma, R. D. Komistek, and H. E. Cates, “Single versus multiple-radii cruciate-retaining total knee arthroplasty: An in vivo mobile fluoroscopy study,” *The Journal of arthroplasty*, 2015.
- [4] S. Nakamura, H. Ito, H. Yoshitomi, S. Kuriyama, R. D. Komistek, and S. Matsuda, “Analysis of the flexion gap on in vivo knee kinematics using fluoroscopy,” *The Journal of arthroplasty*, vol. 30, no. 7, pp. 1237–1242, 2015.
- [5] A. Navacchia, P. J. Rullkoetter, P. Schütz, R. B. List, C. K. Fitzpatrick, and K. B. Shelburne, “Subject-specific modeling of muscle force and knee contact in total knee arthroplasty,” *Journal of Orthopaedic Research*, 2016.
- [6] M. Akter, A. J. Lambert, M. R. Pickering, J. M. Scarvell, and P. N. Smith, “3d ct to 2d low dose single-plane fluoroscopy registration algorithm for in-vivo knee motion analysis,” in *Engineering in Medicine and Biology Society (EMBC), 2014 36th Annual International Conference of the IEEE*, pp. 5121–5124, IEEE, 2014.

- [7] S. A. Banks and W. A. Hodge, “Accurate measurement of three-dimensional knee replacement kinematics using single-plane fluoroscopy,” *Biomedical Engineering, IEEE Transactions on*, vol. 43, no. 6, pp. 638–649, 1996.
- [8] M. R. Mahfouz, W. A. Hoff, R. D. Komistek, and D. A. Dennis, “A robust method for registration of three-dimensional knee implant models to two-dimensional fluoroscopy images,” *Medical Imaging, IEEE Transactions on*, vol. 22, no. 12, pp. 1561–1574, 2003.
- [9] A. Prins, B. Kaptein, S. Banks, B. Stoel, R. Nelissen, and E. Valstar, “Detecting condylar contact loss using single-plane fluoroscopy: A comparison with in vivo force data and in vitro bi-plane data,” *Journal of biomechanics*, vol. 47, no. 7, pp. 1682–1688, 2014.
- [10] “Journey II BCS.” http://www.smith-nephew.com/global/assets/pdf/products/surgical/journey_product.pdf. Accessed: 2016-05-06.
- [11] “Sawbones.” <http://www.sawbones.com/>. Accessed: 2016-05-06.
- [12] E. S. Grood and W. J. Suntay, “A joint coordinate system for the clinical description of three-dimensional motions: application to the knee,” *Journal of biomechanical engineering*, vol. 105, no. 2, pp. 136–144, 1983.
- [13] J. Canny, “A computational approach to edge detection,” *Pattern Analysis and Machine Intelligence, IEEE Transactions on*, no. 6, pp. 679–698, 1986.
- [14] “Jointtrack.” <http://sourceforge.net/projects/jointtrack/>.
- [15] B. J. Fregly, H. A. Rahman, and S. A. Banks, “Theoretical accuracy of model-based shape matching for measuring natural knee kinematics with single-plane fluoroscopy,” *Journal of biomechanical engineering*, vol. 127, no. 4, pp. 692–699, 2005.
- [16] J. Smis and S. De Coninck, “Modeling of UGent Knee Simulator,” Master’s thesis, Ghent University, Belgium, 2015.
- [17] D. A. Forsyth and J. Ponce, “A modern approach,” *Computer Vision: A Modern Approach*, pp. 88–101, 2003.

- [18] J. H. Hubbell and S. M. Seltzer, “Tables of x-ray mass attenuation coefficients and mass energy-absorption coefficients 1 keV to 20 MeV for elements $Z=1$ to 92 and 48 additional substances of dosimetric interest,” tech. rep., National Inst. of Standards and Technology-PL, Gaithersburg, MD (United States). Ionizing Radiation Div., 1995.